

Analysis of Brain White Matter via Fiber Tract Modeling

^{1,2}Guido Gerig, ^{2,3}Sylvain Gouttard, and ^{1,2}Isabelle Corouge

¹Department of Computer Science, ²Department of Psychiatry
University of North Carolina, Chapel Hill, NC 27599, USA

³ESCPE Lyon, 69100 Villeurbanne, France

email: gerig@cs.unc.edu

Abstract— White matter fiber bundles of the human brain form a spatial pattern defined by the anatomical and functional architecture. Tractography applied to the tensor field in diffusion tensor imaging (DTI) results in sets of streamlines which can be associated with major fiber tracts. Comparison of fiber tract properties across subjects needs comparison at corresponding anatomical locations. Moreover, clinical analysis studying fiber tract disruption and integrity requires analysis along tracts and within cross-sections, which is hard to accomplish by conventional region of interest and voxel-based analysis. We propose a new framework for MR DTI analysis that includes tractography, fiber clustering, alignment via local shape parametrization and diffusion analysis across and along tracts. Feasibility is shown with the uncinate fasciculus and the cortico-spinal tracts. The extended set of features including fiber tract geometry and diffusion properties might lead to an improved understanding of diffusion properties and its association to normal/abnormal brain development.

I. INTRODUCTION

Diffusion Tensor Imaging (DTI) measures local probability distribution of the self-motion of water molecules. Restricted motion of extra- and intra-cellular fluid within brain white matter fibers correlates local diffusion patterns, in its simplest form represented by local tensors, with the orientation and density of white matter fibers. The potential of DTI to present white matter integrity, disruption and pathology long before visible changes occur in structural imaging makes it the preferred modality to study white matter diseases. The two tensor measures most commonly used in clinical analysis are the “apparent diffusion coefficient” (ADC, trace of tensor) and the “fractional anisotropy” (FA, normalized difference from spherical). Previous research has been mostly focused on the robust calculation of the tensor field, regularization [1], scientific visualization [2] and fiber tracking [3], [4], [5], [6], [7], [8]. Atlas building and comparison of subject groups have been studied by non-linear registration of DTI images [9] and by combining tractography and spatial normalization [10].

Clinical analysis of DTI mostly followed the common concept of aligning DTI images via affine transformation to a template and statistical parametric mapping (SPM) for voxel-wise group difference tests [11], [12], [13]. Despite the use of manually defined regions of interest, discussion of results used the terms “connectivity” and “fiber disruption”, properties that might be better explained by modeling of whole tracts. Kubicki *et al.* [12], [13] report about differences of cross-sectional area of the uncinate fasciculus and the cingulate, measured in orthogonal sections of the MRI acquisition. They could further show significant

differences between controls and schizophrenics using the fractional anisotropy area statistics. These studies show that clinical analysis of DTI could benefit from improved tools for reliable extraction of fiber tracts of interest, for establishing homology across subjects, and for measuring and comparing geometric and diffusion properties along tracts. This paper significantly extends earlier work initiated by Fillard *et al.* [8] and by Corouge *et al.* [14]. We will not describe tractography but focus on the subsequent quantitative analysis.

II. QUANTITATIVE ANALYSIS OF WHITE MATTER FIBER TRACTS

We have developed a new set of tools for quantitative analysis of diffusion properties associated with fiber tracts:

- Tractography to extract sets of streamlines representing major fiber tracts.
- Fiber bundling and outlier removal.
- Parametrization of sets of streamlines representing bundles.
- Calculation of local parameters of space curves to help to establish point to point correspondence between tracts.
- Calculation of diffusion properties within bundle cross-sections and along bundles.
- Statistical analysis of fiber tract properties across subjects.

The following subsections summarize the individual processing steps, more details are found in [14]. Figure 2 illustrates the concept with the example of the uncinate fasciculus. The complexity of the structure indicates that it might be difficult to measure properties with region of interest analysis. We used tractography and clustering to extract the left and the right bundles, parametrized the set of streamlines and attribute each line with a parameter extracted from the local diffusion tensors, here the fractional anisotropy (Fig. 2 lower right).

A. Tractography

The extraction of sets of streamlines from the diffusion tensor field is performed with a method originally developed by Mori *et al.* [15] and further improved by Fillard *et al.* [8]¹. Selection of source and target regions is similar to the concept outlined in [15]; we use backtracking from target to source and use large target regions (the full brain or the whole portion superior to the corpus callosum, e.g.) to generate seed points to be traced back to the source region.

¹Fiber tracking tool download at <http://www.cs.unc.edu/~fillard>

Tracking is regularized by two parameters controlling local coherence and smoothness of streamlines. Results for a set of major tracts are shown in Fig. 1a.

B. Clustering of curves to bundles

Tractography results in sets of streamlines connecting target to source regions. As our tracking is not guided by geometric constraints, this set can be noisy and can include multiple paths (see Fig. 3a,b and d). We developed a clustering scheme that uses various curve distance metrics to remove outliers and to combine curves to bundles. Closely related previous work has been proposed by Ding *et al.* [16]. Their bundling algorithm relies on the concept of subdivision into curve segments and the use of Euclidean distance to define similarity centered around a core curve. We extend this notion of *cable-like bundles* in order to represent *ribbon cables* and even bundles represented by *sweeping* a template curve to form a manifold [14], using the full set of pairwise distances.

The fiber tracking process provides us with a set \mathcal{F} of 3D curves, F_i , each represented by a set of 3D points \mathbf{p}_k , $\mathcal{F} = \{F_i, F_i = \{\mathbf{p}_k\}\}$. Given a pairwise distance d and a fiber F_i , d is computed between F_i and F_j for all F_j in \mathcal{F} , $j \neq i$. F_i and F_j are decided to be in the same class if $d(F_i, F_j) < t$ where $t \in \mathbb{R}$ is a threshold to be chosen. This process can be described as a graph clustering. A graph with nodes representing the curves and attributed edges representing pairwise distance is cut at threshold t , breaking the whole graph into a number of clusters. Each cluster is populated with a number of curves. Clusters of very low cardinality (e.g. containing less than 10% of initial fibers) are considered as outliers and rejected. Thus, for each fiber F_i within a class \mathcal{C} , at least one fiber $F_j, j \neq i$ in \mathcal{C} is such that $d(F_i, F_j) < t$. In our implementation, we calculate a matrix of pairwise distances where each curve gets an individual label. These labels are iteratively propagated to neighbors until there is no change. This clustering possesses a “transitivity property” and can also collect sets of curves which are not close to one single template but which can be described as a continuous sweeping of curves across space. Only one parameter, the threshold t , has to be selected. A large value of t results in a small number of classes, whereas a smaller value will increase the number of classes. The optimal parameter t depends on the data set under examination and on the choice of the distance metric. We compute the histogram of the number of classes as a function of t to study the sensitivity of each metric in regard to this parameter and to guide users to come up with a meaningful choice. For example, users can select the number of sought clusters instead of the parameter itself, which is used in Figure 3d to separate left and right cortico-spinal tracts.

Three pairwise distances between curves F_i and F_j have been implemented:

1. Closest point distance d_c : Closest distance between pairs of curves A and B.
2. Mean d_M of closest distances: Mean of closest distance for every point of curve A to curve B.

3. Hausdorff distance, d_H : Maximum of point-wise minimum distances between pairs of curves.

Since all these distances are not symmetric, we calculate the combined metrics for A to B and B to A. Additionally, we use shape-based distances by extracting geometric characteristics from fibers such as length, center of mass and second order moments. The principle of the clustering algorithm remains the same when using first or second order moments. In the former case, d is the Euclidean distance between centers of mass, called d_G , whereas in the latter case it represents orientation similarity of the first principal directions.

The overall closest distance d_c can not be expected to have a good discrimination power between fibers since a single closest point pair does not encode shape similarity. On the contrary, d_M provides a global similarity measure since it integrates closest distances along the whole curve. The Hausdorff distance is a worst-case distance, it is a useful metric to reject outliers and prevents the algorithm from clustering curves with high dissimilarity. Centers of mass are an appropriate feature to measure coarse similarity of pose since they are a first order complete representation of a fiber, whereas the second order moment metric has difficulties to discriminate dense fiber sets because of its noise sensitivity.

The interactively guided clustering allows a multi-criteria based classification. For example, outliers can be first rejected based on length and Hausdorff distance whereas left/right bundles might be separated by comparing the center of mass. We will develop guidelines for major tracts and thus standardize the procedure aiming towards an automated clustering scheme.

C. Attributing bundles with diffusion properties

It is now interesting to study local diffusion not in small regions of interest but as a function of the geometry of the whole tract. Our tractography tool [8] simplifies this task since fibers are stored as standardized ITK poly-lines attributed with the full tensor and derived properties. Visualization of the splenium (Fig. 1b) clearly demonstrates that the fractional anisotropy varies significantly as a function of location along the tract but also within cross-sections. The histogram representing the mid-sagittal cross-section (Fig. 1c) clearly shows that values range from 0.1 up to 0.9, representing the whole range from nearly isotropic up to highly anisotropic diffusion. We assume that this broad range is a function of the coarse sampling of the underlying macroscopic fiber structures (here $2 \times 2 \times 2 \text{mm}^3$), partial voluming, but also natural variation of fiber density and myelination sheath. However, it demonstrates that region of interest analysis is not sufficient and might be very sensitive to the exact definition of cross-sections.

DTI properties of large bundles (corpus callosum and cortico-spinal) are illustrated in the first column of Fig. 5. Whereas apparent diffusion (ADC) is mostly constant across the whole bundle, an interesting pattern is observed in fractional anisotropy (FA). The FA values change signif-

icantly and form regular patterns. The dark blue on top is easily explained by fiber dispersion towards the cortex and thus isotropic diffusion. The “stripe” patterns are induced by neighboring tracts either running in parallel or perpendicular. These views again indicate that regions of interest analysis might not capture this natural variation and even might be very sensitive to selecting locations along tracts.

D. Parametrization of fiber bundles

Summarizing diffusion properties within a bundle requires parametrization. First, we define a common origin for the set of fibers in each cluster. The choice of this origin might be based on geometric criteria, e.g. a cross-section with minimal area, or based on anatomical information, like the symmetry plane of the interhemispheric fissure. The polyline of each curve is parametrized by a cubic B-spline curve. The set of splines is re-sampled and diffusion measurements at each point are obtained by interpolation. The two attributes ADC and FA can now be integrated across cross-sections and expressed as a function of arc-length. Fig. 5 displays average and standard deviations of ADC and along the fiber directions, i.e. from inferior to superior direction. Results are illustrated for a healthy adult case. The curves representing FA clearly reflect the “stripes” shown in the color displays, and also indicate that the commonly used region of interest analysis need high spatial precision not to be affected by this large natural variations.

E. Attributing bundles with local shape properties

Comparison of fiber tracts across subjects requires a one-to-one correspondence between tracts. We explore the use of local shape statistics on the set of curves to automatically and reproducibly define significant locations along tracts. Given a differentiable parametrization $r(t)$ of a curve \mathcal{C} , we calculate the Frénet frame $(\vec{T}, \vec{N}, \vec{B})$ in each point \mathbf{p} of the curves.

The vector \vec{T} is the unit tangent vector, \vec{N} the unit normal vector and \vec{B} supplements the frame so that it is orthonormal. At each point \mathbf{p} , this frame allows the calculation of local features such as curvature κ and torsion τ . We use the parametrization by cubic B-splines as discussed earlier to establish point correspondence between sets of fibers. Points with the same curvilinear abscissæ across the fiber set, i.e. with the same arc-length, are defined as homologous. Results for curvature of the corpus callosum bundle are shown in Fig. 4. The mesh representations and the mean and standard deviation of curvature reflect the high similarity of the U-shaped curves close to the origin (midsagittal plane) and the increased variability towards the cortex (left and right in graphs) as expected due to fiber dispersion.

III. CONCLUSION

This paper discussed work in progress for quantitative analysis of DTI data. Unlike voxel-based analysis by non-linear registration, we develop a “tract-based” concept that uses tractography to define complex regions of interest.

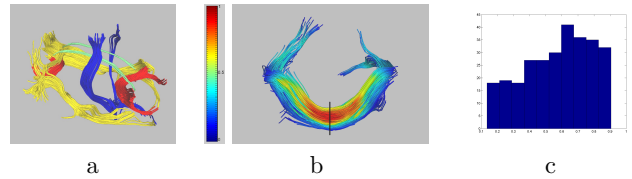


Fig. 1. DTI fiber tracts: a) Sets of tracts obtained by tractography, b) coloring FA properties along and across bundle (range $[0 \dots 1]$ represented from blue to red) and c) histogram of FA properties within mid-sagittal cross-section.

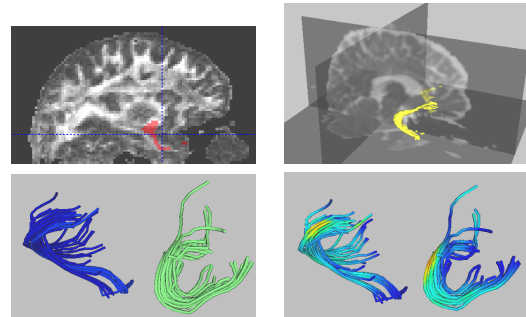


Fig. 2. Uncinate fasciculus: Top: Sagittal cut with overlay of segmented structure and three-dimensional view of left and right uncinate. Bottom: Left and right fasciculi obtained by fiber tracking and same structures but color-coding of FA value.

Tracts are parametrized and attributed with local diffusion properties and local shape characteristics. This allows us to calculate diffusion properties within cross-sections and along bundles. This analysis will naturally complement the currently used whole brain screening by alignment and SPM statistics. For example, regions of interest found as significant could be used to focus on specific tracts using the method proposed here. The preliminary analysis and visualization clearly demonstrates that diffusion tensor properties change significantly across bundles but also along tracts. This observation also raises the question of currently used parametric statistics (e.g. mean FA) within regions of interest are appropriate. The few cases illustrated in this paper are part of two much larger studies which a) explore normal variability within a set of 15 healthy adults and b) study early brain development of newborns at risk (age 2 weeks) with follow-up after 1 and/or 2 years. Models on healthy controls will help us to



Fig. 3. Clustering of sets of streamlines to fiber bundles. Cortico-spinal tract before and after clustering.

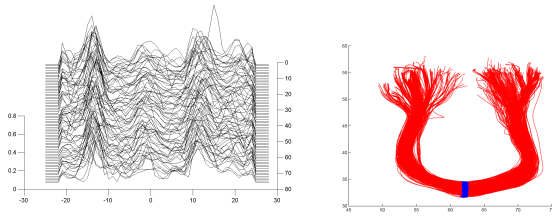


Fig. 4. Local shape properties along callosal tract. Left: Mesh display of curvature along tracts illustrating curvature (left to right) for the set of fibers (front to back). Right: Callosal tract with center of origin

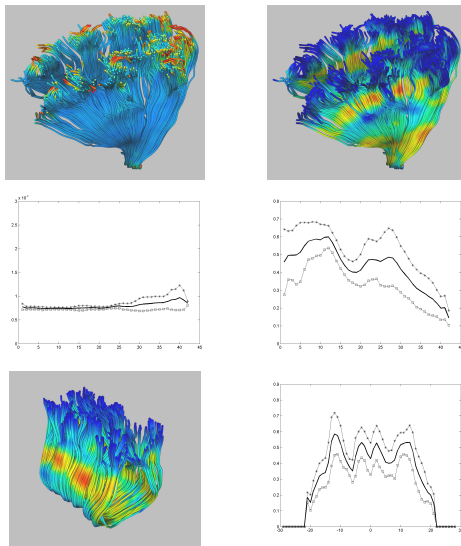


Fig. 5. Analysis of diffusion properties along major fiber tracts. Top: ADC and FA values for the cortico-spinal tracts, bottom row FA for the callosal tract. Middle: Corresponding statistics, left to right represents inferior to superior and the vertical axis the ADC and FA values. Mean and standard deviations are shown. Bottom: Corpus callosum tract with FA color coding and corresponding statistics.

measure and quantify geometric and diffusion changes of fiber tracts due to pathology.

Acknowledgement

This research is supported by the NIH NIBIB grant P01 EB002779, the NIH Conte Center MH064065, and the Stanley Medical Research Institute. We acknowledge Matthieu Jomier and Julien Jomier, both UNC-Chapel Hill, for their precious help, fruitful discussions and support with software development.

REFERENCES

[1] T. McGraw, B.C. Vemuri, Z. Wang, Y. Chen, M. Rao, and T. Mareci, "Line integral convolution for visualization of fiber tract maps from DTI," in *Medical Image Computing and Computer Assisted Intervention [MICCAI02]*, T. Dohi and R. Kikinis, Eds. August 2002, vol. 2489 of *Lecture Notes in Computer Science LNCS*, pp. 615–622, Springer Verlag.

[2] Abhir Bhalerao and Carl-Fredrik Westin, "Tensor splats: Visualising tensor fields by texture mapped volume rendering," in *Medical Image Computing and Computer Assisted Analysis*

MICCAI. 2003, Lecture Notes in Computer Science LNCS, pp. 294–302, Springer.

[3] C.-F. Westin, S.E. Maier, H. Mamata, A. Nabavi, F.A. Jolesz, and R. Kikinis, "Processing and visualization for diffusion tensor MRI," *Medical Image Analysis*, vol. 6, pp. 93–108, 2002.

[4] O. Coulon, D.C. Alexander, and S.R. Arridge, "A regularization scheme for diffusion tensor magnetic resonance images," in *Proc. Information Processing in Medical Imaging*, M.F. Insana and R.M. Leahy, Eds. 2001, vol. 2082 of *Lecture Notes in Computer Science*, pp. 92–105, Springer-Verlag.

[5] P.J. Basser, S. Pajevic, C. Pierpaoli, and A. Aldroubi, "Fiber tract following in the human brain using DT-MRI data," *IEICE Trans. on Information and Systems*, vol. E85-D, no. 1, pp. 15–21, 2002.

[6] M. Björnemo, A. Brun, R. Kikinis, and C.-F. Westin, "Regularized stochastic white matter tractography using diffusion tensor MRI," in *Proc. of Medical Image Computing and Computer-Assisted Intervention*, T. Dohi and R. Kikinis, Eds. 2002, vol. 2488 of *Lecture Notes in Computer Science*, pp. 435–442, Springer-Verlag.

[7] L. Zhukov and A.H. Barr, "Oriented tensor reconstruction: tracing neural pathways from diffusion tensor MRI," in *Proc. IEEE Visualization*, 2002.

[8] P. Fillard and G. Gerig, "Analysis tool for diffusion tensor MRI," in *Proc. of Medical Image Computing and Computer-Assisted Intervention*, 2003, vol. 2879 of *Lecture Notes in Computer Science*, pp. 967–968.

[9] D.C. Alexander and J.C. Gee, "Elastic matching of diffusion tensor images," *Computer Vision and Image Understanding*, vol. 77, pp. 233–250, 2000.

[10] D. Xu, S. Mori, M. Solaiyappan, P.C.M. van Zijl, and C. Davatzikos, "A framework for callosal fiber distribution analysis," *NeuroImage*, vol. 17, pp. 1131–1143, 2002.

[11] K.O. Lim, M. Hedehus, M. Moseley, A. de Crespigny, E.V. Sullivan, and A. Pfefferbaum, "Compromised white matter tract integrity in schizophrenia inferred from diffusion tensor imaging," *Archives of General Psychiatry*, vol. 56, pp. 367–374, 1999.

[12] M. Kubicki, C.F. Westin, S.E. Maier, M. Frumin, P.G. Nestor, and D.F. Salisbury, "Uncinate fasciculus findings in schizophrenia: a magnetic resonance diffusion tensor imaging study," *American Journal of Psychiatry*, vol. 159, pp. 813–820, 2002.

[13] M. Kubicki, C.F. Westin, R. McCarley, C. Wible, M. Frumin, and S. Maier, "Cingulate fasciculus integrity disruption in schizophrenia: a magnetic resonance diffusion tensor imaging study," *Biol Psychiatry*, vol. 54, pp. 1171–1180, 2003.

[14] I. Corouge, S. Gouttard, and G. Gerig, "Towards a shape model of white matter fiber bundles using diffusion tensor MRI," in *IEEE Proceedings Int. Symposium Biomedical Imaging. IEEE Computer Society Press*, 2004, in print.

[15] S. Mori, W.E. Kaufmann, C. Davatzikos, B. Stieltjes, L. Amodoi, K. Fredericksen, G.D. Pearlson, E.R. Melhem, M. Solaiyappan, G.V. Raymond, H.W. Moser, and van Zijl P.C.M., "Imaging cortical association tracts in the human brain using diffusion-tensor-based axonal tracking," *Magnetic Resonance in Medicine*, vol. 47, pp. 215–223, 2002.

[16] Z. Ding, J.C. Gore, and A.W. Anderson, "Classification and quantification of neuronal fiber pathways using diffusion tensor MRI," *Magnetic Resonance in Medicine*, vol. 49, pp. 716–721, 2003.

[17] Guihuao Zhai, Weili Lin, Kathy Wilber, Guido Gerig, and John H. Gilmore, "Comparison of regional white matter diffusion in healthy neonates and adults using a 3T head-only MR scanner," *Radiology*, vol. 229, pp. 673–681, DEC 2003.